

---

MARTIN–LUTHER–UNIVERSITÄT  
HALLE–WITTENBERG  
INSTITUT FÜR MATHEMATIK



---

**Implicit-Explicit Peer Methods**

**B. Soleimani, O. Knoth and R. Weiner**

**Report No. 04 (2016)**

---

**Editors:**

Professors of the Institute for Mathematics, Martin Luther University Halle-Wittenberg.

**Electronic version:** see <http://www.mathematik.uni-halle.de/institut/reports/>

# Implicit-Explicit Peer Methods

B. Soleimani, O. Knoth and R. Weiner

Report No. 04 (2016)

Behnam Soleimani  
Rüdiger Weiner

Martin-Luther-Universität Halle-Wittenberg  
Naturwissenschaftliche Fakultät II  
Institut für Mathematik  
Theodor-Lieser-Str. 5  
D-06120 Halle/Saale, Germany

Email: [behnam.soleimani@mathematik.uni-halle.de](mailto:behnam.soleimani@mathematik.uni-halle.de)  
[ruediger.weiner@mathematik.uni-halle.de](mailto:ruediger.weiner@mathematik.uni-halle.de)

Oswald Knoth

Leibniz-Institut für Troposphärenforschung e.V. (TROPOS)  
Permoserstraße 15  
D-04318 Leipzig, Germany

Email: [oswald.knoth@tropos.de](mailto:oswald.knoth@tropos.de)



# Implicit-Explicit Peer Methods

B. Soleimani, O. Knoth and R. Weiner

July 12, 2016

## Abstract

Differential equations with both stiff and nonstiff parts can be solved efficiently by implicit-explicit (IMEX) methods. There have been considered various approaches in the literature. In this paper we introduce IMEX peer methods. We show that the combination of an explicit with an implicit peer method, both of order  $p$ , gives an IMEX peer method of the same order. We construct methods of orders 3 and 4 with respect to stability requirement of fast-wave-slow-wave problems. Numerical tests and comparisons with other methods for problems from weather prediction show the high potential of IMEX peer methods.

**Keywords.** Partitioned peer methods, IMEX peer methods, stability.

## 1 Introduction

Many problems in engineering, physics, chemistry and other areas involve the numerical solution of time-dependent partial differential equations (PDEs). By spatial discretization the PDEs can be transformed into large systems of ordinary differential equations which can include both stiff and nonstiff parts:

$$y' = f(t, y) + g(t, y), \quad y(t_0) = y_0. \quad (1)$$

Here  $f$  is the stiff and  $g$  is the nonstiff part. An appropriate strategy is treating the stiff part by implicit methods because the step size is not limited by stability requirements and the nonstiff part by explicit methods because of their low cost per step. IMEX methods have been considered intensively in the literature [1, 6, 7, 24, 25]. Here we treat the stiff part with implicit peer methods [14] and the nonstiff part with explicit peer methods [18]. For more details and properties of implicit peer methods see [2, 3, 5, 11–13] and properties of explicit peer methods can be found in [18, 20].

First we introduce partitioned peer methods and derive order conditions for such methods. Then with the help of partitioned peer methods we introduce IMEX peer methods. This paper is organized as follows:

In Section 2 we introduce  $s$ -stage partitioned peer methods, derive order conditions and consider zero stability and convergence. On the basis of partitioned peer methods in the third section we define IMEX peer methods following the approach of Ascher et.al. [1]. We investigate order of consistency, zero stability and convergence properties. In Section 4, we discuss the stability properties of IMEX peer methods with respect to typical test equation from weather prediction [21] and another linear test equation which is frequently used in the literature [24, 25]. Furthermore we construct special IMEX peer methods of order  $p = s$ , where the implicit part is A-stable and give the coefficients of two methods of order 3 and 4 used in the numerical tests. At the end of the fourth section, we investigate the stability properties of the derived IMEX peer methods with respect to the above mentioned test equations. In the fifth section, we compare our methods with other methods on problems from weather prediction like two dimensional nonlinear gravity waves and the cold bubble downburst benchmark example.

## 2 Partitioned peer methods

Suppose that the system of differential equation is partitioned as follows:

$$y' = \begin{pmatrix} u' \\ v' \end{pmatrix} = \begin{pmatrix} f(t, u, v) \\ g(t, u, v) \end{pmatrix}, \quad (2)$$

where  $y$  is separated into two components  $u$  and  $v$ . Here  $u' = f$  is the stiff and  $v' = g$  is the nonstiff part. The stiff part will be treated by an implicit and the nonstiff part by an explicit peer method. Then an  $s$ -stage partitioned peer method is given by (for simplicity of notation for scalar equations):

$$\begin{aligned} U_m &= BU_{m-1} + h_m AF(t_{m-1}, U_{m-1}, V_{m-1}) + h_m RF(t_m, U_m, V_m), \\ V_m &= \widehat{B}V_{m-1} + h_m \widehat{A}G(t_{m-1}, U_{m-1}, V_{m-1}) + h_m \widehat{R}G(t_m, U_m, V_m). \end{aligned} \quad (3)$$

with matrices  $A, \widehat{A}, B, \widehat{B}, R, \widehat{R} \in R^{s \times s}$ ,  $c = (c_1, c_2, \dots, c_{s-1}, 1)$ ,  $U_m = (U_{m,1}, \dots, U_{m,s})$ ,  $V_m = (V_{m,1}, \dots, V_{m,s})$  and

$$R = \begin{pmatrix} \gamma & & & & \\ * & \gamma & & & \\ * & * & \gamma & & \\ * & * & * & \gamma & \\ * & * & * & * & \gamma \end{pmatrix}, \quad \widehat{R} = \begin{pmatrix} 0 & & & & \\ * & 0 & & & \\ * & * & 0 & & \\ * & * & * & 0 & \\ * & * & * & * & 0 \end{pmatrix},$$

$$F_m = F(t_m, U_m, V_m) = \begin{pmatrix} f_1(t_{m,1}, U_{m,1}, V_{m,1}) \\ f_2(t_{m,2}, U_{m,2}, V_{m,2}) \\ \vdots \\ f_s(t_{m,s}, U_{m,s}, V_{m,s}) \end{pmatrix}, \quad G_m = G(t_m, U_m, V_m) = \begin{pmatrix} g_1(t_{m,1}, U_{m,1}, V_{m,2}) \\ g_2(t_{m,2}, U_{m,2}, V_{m,2}) \\ \vdots \\ g_s(t_{m,s}, U_{m,s}, V_{m,s}) \end{pmatrix}.$$

Here  $t_{m,i} = t_m + c_i h_m$  and the stage solutions  $U_{m,i}, V_{m,i}$  are approximations to the exact solutions  $u(t_m + c_i h_m), v(t_m + c_i h_m), i = 1, 2, \dots, s$ . We always assume that the nodes  $c_i$  are constant and pairwise distinct. Note that the coefficients will depend on the step size ratio  $\sigma_m = h_m/h_{m-1}$  in general.

Explicit and implicit peer methods were studied in a series of papers and adapted to special properties like parallelism or application with Krylov techniques for high dimensional problems e.g. [2, 3, 5, 11–13, 20].

## 2.1 Order conditions

Order conditions can be derived by substituting the exact solution into the method and making a Taylor expansion of the residual  $\Delta_{mi}$ .

**Theorem 2.1.** *If the coefficients of the partitioned peer method (3) satisfy the conditions  $AB(l) = \widehat{AB}(l) = 0$ , where*

$$AB_i(l) = c_i^l - \sum_{j=1}^s b_{ij} \frac{(c_j - 1)^l}{\sigma_m^l} - l \sum_{j=1}^s a_{ij} \frac{(c_j - 1)^{l-1}}{\sigma_m^{l-1}} - l \sum_{j=1}^i r_{ij} c_j^{l-1},$$

$$\widehat{AB}_i(l) = c_i^l - \sum_{j=1}^s \widehat{b}_{ij} \frac{(c_j - 1)^l}{\sigma_m^l} - l \sum_{j=1}^s \widehat{a}_{ij} \frac{(c_j - 1)^{l-1}}{\sigma_m^{l-1}} - l \sum_{j=1}^i \widehat{r}_{ij} c_j^{l-1},$$

for all  $l = 0, \dots, p$  and  $i = 1, \dots, s$ , then method (3) is consistent of order  $p$ .

*Proof.* By Taylor expansion, we get

$$\begin{aligned} \Delta_{mi} &= \begin{pmatrix} u(t_{m,i}) \\ v(t_{m,i}) \end{pmatrix} - \sum_{j=1}^s \begin{pmatrix} b_{ij} u(t_{m-1,j}) \\ \widehat{b}_{ij} v(t_{m-1,j}) \end{pmatrix} - h_m \sum_{j=1}^s \begin{pmatrix} a_{ij} u'(t_{m-1,j}) \\ \widehat{a}_{ij} v'(t_{m-1,j}) \end{pmatrix} - h_m \sum_{j=1}^i \begin{pmatrix} r_{ij} u'(t_{m,j}) \\ \widehat{r}_{ij} v'(t_{m,j}) \end{pmatrix} \\ &= \begin{pmatrix} \sum_{l=0}^p (c_i^l - \sum_{j=1}^s b_{ij} \frac{(c_j-1)^l}{\sigma_m^l} - l \sum_{j=1}^s a_{ij} \frac{(c_j-1)^{l-1}}{\sigma_m^{l-1}} - l \sum_{j=1}^i r_{ij} c_j^{l-1}) \frac{h_m^l}{l!} u^{(l)}(t_m) \\ \sum_{l=0}^p (c_i^l - \sum_{j=1}^s \widehat{b}_{ij} \frac{(c_j-1)^l}{\sigma_m^l} - l \sum_{j=1}^s \widehat{a}_{ij} \frac{(c_j-1)^{l-1}}{\sigma_m^{l-1}} - l \sum_{j=1}^i \widehat{r}_{ij} c_j^{l-1}) \frac{h_m^l}{l!} v^{(l)}(t_m) \end{pmatrix} + \begin{pmatrix} O(h_m^{p+1}) \\ O(h_m^{p+1}) \end{pmatrix} \end{aligned}$$

and therefore we have order  $p$  if  $AB(l) = \widehat{AB}(l) = 0$  is satisfied for  $l = 0, \dots, p$ .  $\square$

**Remark 2.2.** *For  $l = 0$ , we get  $1 - \sum_{j=1}^s b_{ij} = 0$  and  $1 - \sum_{j=1}^s \widehat{b}_{ij} = 0$ , i.e.  $B\mathbf{1} = \widehat{B}\mathbf{1} = \mathbf{1}$ , implying preconsistency.*

**Remark 2.3.** *The residuals of all stages are of the same order. Therefore the stage order  $q$  of peer methods is equal to the order of consistency  $p$ .*

**Corollary 2.4.** *The partitioned peer method (3) is consistent of order  $p = s$  if  $B\mathbb{1} = \widehat{B}\mathbb{1} = \mathbb{1}$  and*

$$A_m = (CV_0 - RV_0D)D^{-1}S_mV_1^{-1} - \frac{1}{\sigma_m}B(C - I)V_1D^{-1}V_1^{-1} \quad (4)$$

$$\widehat{A}_m = (CV_0 - \widehat{R}V_0D)D^{-1}S_mV_1^{-1} - \frac{1}{\sigma_m}\widehat{B}(C - I)V_1D^{-1}V_1^{-1}, \quad (5)$$

where  $V_0 = (c_i^{j-1})_{i,j=1}^s$ ,  $V_1 = ((c_i - 1)^{j-1})_{i,j=1}^s$ ,  $D = \text{diag}(1, \dots, s)$ ,  $S_m = \text{diag}(1, \sigma_m, \dots, \sigma_m^{s-1})$  and  $C = \text{diag}(c_i)$ .

This means that for arbitrary coefficient matrices  $R, \widehat{R}$  and  $B, \widehat{B}$  satisfying the preconsistency conditions  $B\mathbb{1} = \widehat{B}\mathbb{1} = \mathbb{1}$ , the computation of  $A_m$  and  $\widehat{A}_m$  by (4) and (5) guarantees order of consistency  $p = s$ .

**Definition 2.5.** *The partitioned peer method (3) is called zero-stable if there exists a constant  $K > 0$  such that for all  $m, l \geq 0$  holds*

$$\left\| \prod_l \begin{pmatrix} B_{m+l} \cdots B_{m+1} B_m & 0 \\ 0 & \widehat{B}_{m+l} \cdots \widehat{B}_{m+1} \widehat{B}_m \end{pmatrix} \right\| \leq K.$$

We will consider constant matrices  $B$  and  $\widehat{B}$ . In this case the peer method (3) is zero-stable if the eigenvalue  $\lambda_i$  and  $\widehat{\lambda}_i$  of  $B$  and  $\widehat{B}$  have modulus less or equal one and all eigenvalues of modulus one are simple. If  $\lambda_1 = \widehat{\lambda}_1 = 1$  and  $\lambda_i = \widehat{\lambda}_i = 0$  for  $i = 2, \dots, s$ , then the method is called optimally zero-stable.

**Theorem 2.6.** *Let  $B, \widehat{B}, R, \widehat{R}$  in (3) be constant matrices,  $h := \max_m h_m$ ,  $\max_m \sigma_m \leq \sigma_{\max}$ . Let  $B\mathbb{1} = \widehat{B}\mathbb{1} = \mathbb{1}$  and let the method be zero-stable. Let the error of the starting values satisfy  $\varepsilon_0 = \mathcal{O}(h_0^s)$  and let  $A_m$  and  $\widehat{A}_m$  be given by (4) and (5). Then the method (3) is convergent of order  $p = s$ .*

*Proof.* Without loss of generality, we consider the autonomous case. Let  $\Delta_m = \begin{pmatrix} \overline{\Delta}_m \\ \widehat{\Delta}_m \end{pmatrix}$ . The global error can be written in the form:

$$\begin{aligned} \varepsilon_m &= \begin{pmatrix} \overline{\varepsilon}_m \\ \widehat{\varepsilon}_m \end{pmatrix} = \begin{pmatrix} U(t_m) - U_m \\ V(t_m) - V_m \end{pmatrix} \\ &= \begin{pmatrix} U(t_m) - BU_{m-1} - h_m A_m F(U_{m-1}, V_{m-1}) - h_m R F(U_m, V_m) \\ V(t_m) - \widehat{B}V_{m-1} - h_m \widehat{A}_m G(U_{m-1}, V_{m-1}) - h_m \widehat{R} G(U_m, V_m) \end{pmatrix} \\ &= \begin{pmatrix} B\overline{\varepsilon}_{m-1} \\ \widehat{B}\widehat{\varepsilon}_{m-1} \end{pmatrix} + \begin{pmatrix} h_m A_m (F(U(t_{m-1}), V(t_{m-1}))) - F_{m-1} + h_m R (F(U(t_m), V(t_m)) - F_m) + \overline{\Delta}_m \\ h_m \widehat{A}_m (G(U(t_{m-1}), V(t_{m-1}))) - G_{m-1} + h_m \widehat{R} (G(U(t_m), V(t_m)) - G_m) + \widehat{\Delta}_m \end{pmatrix}. \end{aligned}$$

By zero-stability there exist vector norms  $\|\cdot\|_a$  and  $\|\cdot\|_b$  such that in the induced matrix norms

$$\|B\|_a = \varrho(B) = 1 \quad \text{and} \quad \|\widehat{B}\|_b = \varrho(\widehat{B}) = 1. \quad (6)$$



Then with the norm

$$\left\| \begin{pmatrix} u \\ v \end{pmatrix} \right\| = \max\{\|u\|_a, \|v\|_b\}. \quad (7)$$

we get

$$\begin{aligned} \|\varepsilon_m\| &= \left\| \begin{pmatrix} \bar{\varepsilon}_m \\ \hat{\varepsilon}_m \end{pmatrix} \right\| \leq \left\| \begin{pmatrix} \bar{\varepsilon}_{m-1} \\ \hat{\varepsilon}_{m-1} \end{pmatrix} \right\| + h_m \left\| \begin{pmatrix} A_m(F(U(t_{m-1}), V(t_{m-1}))) - F_{m-1} \\ \hat{A}_m(G(U(t_{m-1}), V(t_{m-1}))) - G_{m-1} \end{pmatrix} \right\| \\ &\quad + h_m \left\| \begin{pmatrix} R(F(U(t_m), V(t_m))) - F_m \\ \hat{R}(G(U(t_m), V(t_m))) - G_m \end{pmatrix} \right\| + \left\| \begin{pmatrix} \bar{\Delta}_m \\ \hat{\Delta}_m \end{pmatrix} \right\|. \end{aligned}$$

By (6) and taking into account the Lipschitz conditions for  $f$  and  $g$  follows

$$\left\| \begin{pmatrix} R(F(U(t_m), V(t_m))) - F_m \\ \hat{R}(G(U(t_m), V(t_m))) - G_m \end{pmatrix} \right\| \leq 2 \max\{\|R\|_a L \|\varepsilon_m\|, \|\hat{R}\|_b \hat{L} \|\varepsilon_m\|\} = d_1 \|\varepsilon_m\|,$$

and

$$\left\| \begin{pmatrix} A_m(F(U(t_{m-1}), V(t_{m-1}))) - F_{m-1} \\ \hat{A}_m(G(U(t_{m-1}), V(t_{m-1}))) - G_{m-1} \end{pmatrix} \right\| \leq d_2 \|\varepsilon_{m-1}\|.$$

By (4) and (5) we have  $\|\bar{\Delta}_m\|_a \leq d_3 h_m^{s+1}$  and  $\|\hat{\Delta}_m\|_b \leq d_4 h_m^{s+1}$  which imply  $\left\| \begin{pmatrix} \bar{\Delta}_m \\ \hat{\Delta}_m \end{pmatrix} \right\| \leq d_5 h_m^{s+1}$ .

We finally get

$$\|\varepsilon_m\| \leq \|\varepsilon_{m-1}\| + h_{m-1} d_6 \|\varepsilon_m\| + h_{m-1} d_7 \|\varepsilon_{m-1}\| + d_8 h_{m-1}^{s+1}$$

and in standard way follows

$$\|\varepsilon_m\| \leq d_9 h_{max}^s + d_{10} \|\varepsilon_0\|.$$

This completes the proof. □

### 3 IMEX methods

Suppose now that our system of ordinary differential equations is modeled as follows:

$$y' = f(t, y) + g(t, y) \quad y(t_0) = y_0, \quad (8)$$

where  $f$  is the stiff part and  $g$  is the nonstiff part. Without loss of generality, we suppose that our system is autonomous. The stiff part will be treated by an implicit peer method and the nonstiff part by an explicit peer method. The system (8) can be transformed into a componentwise partitioned system (2) following the idea of [1, 24] via the transformation

$$\begin{aligned} y &= u + v, \\ u' &= \tilde{f}(u, v) = f(u + v), \\ v' &= \tilde{g}(u, v) = g(u + v). \end{aligned}$$

We choose  $B = \widehat{B}$  and solve this system with the partitioned method (3). Then we get (for simplicity for scalar equations):

$$U_m = BU_{m-1} + h_m AF(U_{m-1} + V_{m-1}) + h_m RF(U_m + V_m), \quad (9)$$

$$V_m = BV_{m-1} + h_m \widehat{A}G(U_{m-1} + V_{m-1}) + h_m \widehat{R}G(U_m + V_m). \quad (10)$$

This yields

$$Y_m = B(Y_{m-1}) + hAF(Y_{m-1}) + hRF(Y_m) + h\widehat{A}G(Y_{m-1}) + h\widehat{R}G(Y_m). \quad (11)$$

Method (11) is called IMEX peer method.

The order conditions follow directly from Theorem 2.1.

**Corollary 3.1.** *The IMEX peer method (11) is consistent of order  $p = s$  if  $B\mathbb{1} = \mathbb{1}$  and if (4), (5) hold with  $B = \widehat{B}$ .*

This means that for arbitrary coefficient matrices  $R, \widehat{R}$  and  $B$  satisfying the preconsistency condition  $B\mathbb{1} = \mathbb{1}$ , the computations of  $A$  and  $\widehat{A}$  by (4) and (5) guarantee order of consistency  $p = s$ . As a consequence of Theorem 2.6 we obtain

**Theorem 3.2.** *Let  $B, R, \widehat{R}$  in (11) be constant matrices,  $h := \max_m h_m$ ,  $\max_m \sigma_m \leq \sigma_{max}$ ,  $\varepsilon_0 = \mathcal{O}(h_0^s)$ , let  $B\mathbb{1} = \mathbb{1}$  and let the IMEX peer method (11) be zero-stable. If additionally  $A_m$  and  $\widehat{A}_m$  are given by (4) and (5) then the method given by (11) is convergent of order  $p = s$ .*

## 4 Stability investigations and construction of IMEX peer methods

In this section, first we discuss the stability properties of IMEX peer methods with respect to typical test equation from weather prediction (fast-wave-slow-waves) and another linear test equation. In fact we applied (11) to the acoustics equations as in [21]. These equations were also used for the optimization of the coefficients in the method search. Furthermore we discuss the stability properties of the IMEX peer methods with respect to the linear test equation considered in [24, 25]. Later we construct special IMEX peer methods of order  $p = s$  and give the coefficients of two methods of order 3 and 4. For these derived methods, we investigate stability properties with respect to the above mentioned test equations and give the stability region with the help of figures.

Our special interest is the application of IMEX peer methods in acoustics equations used in weather prediction models. We therefore here investigate stability properties for this problem class and consider the application of the IMEX peer methods to the acoustics

equation, discretized in space by third order upwind (advection) and central differences on a staggered grid (sound wave terms), cf. [21–23]:

$$\begin{aligned}\mathbf{u}_t &= -c_s \mathbf{p}_x - U \mathbf{u}_x \\ \mathbf{p}_t &= -c_s \mathbf{u}_x - U \mathbf{p}_x,\end{aligned}$$

where  $u$  is the wind speed and  $p$  represents pressure. The two parameters  $c_s$  and  $U$  are the sound speed ( $\approx 340$  m/s) and constant background wind speed respectively, where for this application  $c_s$  is much greater than  $U$ . For later reference, we recall the Mach number which is defined by the quotient of  $U/c_s$ . The common von Neumann stability idea is used for discussing the resulting Fourier modes separately; see [21] for more details of this procedure. We consider the first 20 Fourier modes and obtain for each mode the following split test equation:

$$\dot{y} = Ly + Ny. \quad (12)$$

Here  $N \in \mathbb{C}^{2,2}$  is a diagonal matrix representing the advection part and its eigenvalues are in the left half-plane with comparable imaginary and real parts. The matrix  $L$  is an anti-diagonal matrix coming from the fast part of the linear test equation and its eigenvalues are purely imaginary. Therefore A-stability of the basic implicit method is necessary.

The stability matrix of the IMEX peer method applied to (12) is

$$M(hL, hN) = (I - hLR - hN\hat{R})^{-1}(hLA + hN\hat{A} + B).$$

The test equation (12) is based on the special properties of the acoustics equation. For the application of IMEX methods to general problems with stiff and nonstiff parts, the following test equation is more appropriate:

$$y' = \lambda y + \beta y. \quad (13)$$

This equation is frequently used in literature, see e.g. [24, 25]. Here  $\lambda$  represents the eigenvalues of the Jacobian of the stiff part, and  $\beta$  of the nonstiff part.

Applying the IMEX peer methods to this equation gives

$$Y_m = M(z, \hat{z})Y_{m-1}, \quad M(z, \hat{z}) = (I - zR - \hat{z}\hat{R})^{-1}(zA + \hat{z}\hat{A} + B),$$

where  $z = \lambda h$  and  $\hat{z} = \beta h$ . Note that  $M(0, 0) = B$ .

Suppose that  $S \subset \mathbb{C}$  and  $\hat{S} \subset \mathbb{C}$  are the stability regions of the implicit and the explicit peer method, respectively. The stability region for the IMEX peer method is then defined by

$$\{z \in S, \hat{z} \in \hat{S} : \rho(M(z, \hat{z})) \leq 1\} \subset S \times \hat{S}.$$

Now we construct IMEX peer methods with the following properties:

- Order of consistency  $p = s$ , i.e.  $A_m$  and  $\hat{A}_m$  are computed by (4) and (5).

- Constant coefficient matrix  $B$  satisfying  $B\mathbb{1} = \mathbb{1}$  and to have optimal zero-stability.
- Constant coefficient matrices  $R$  and  $\hat{R}$  with  $r_{ii} = \gamma$ .
- A-stability of the implicit method for constant step sizes.
- Appropriate stability for the linear acoustic equations with a given Mach number. In our case  $1/6$  which is typical for numerical weather forecasting.

We consider the following strategy to construct IMEX peer methods. First we try to find a good implicit method with appropriate properties (optimal zero-stability, A-stability) and establish a proper explicit peer method in way that the combined IMEX peer method has appropriate stability for the linear acoustic equations (12). To find suitable A-stable implicit peer methods we used the MATLAB function *fmincon* with different objective functions and constraints. For example we used order conditions and bounds for  $\rho(M(\infty))$  as constraints and the angle of A-stability as an objective function, but this was too expensive. In another search we added the A-stability condition as constraint and used  $\rho(M(\infty))$  as our objective function. After finding a suitable A-stable implicit peer method, its coefficient matrix  $B$  and nodes  $c$  are used to find an explicit peer method in a way that the combined IMEX peer method has appropriate stability for the linear acoustic equations. Similar to the implicit part, we used the MATLAB function *fmincon* and we tried different strategies. For example, we used order conditions as constraints and stability of the combined method with respect to acoustic equations (12) as an objective function. At the end, we choose the best explicit peer method such that the corresponding IMEX method has appropriate stability for the linear acoustic equations with Mach number  $1/6$ .

We give the coefficients of 2 methods obtained in our search, which have been implemented and tested in MATLAB:

**Method 3a:** p=s=3, A-stable, optimally zero stable

$c_1 = 0.15946593963643907$	$c_2 = 0.54558601055976386$	$c_3 = 1$
$b_{11} = -0.81662611177702749$	$b_{12} = 0.21923402764359148$	$b_{13} = -0.3757141646588873$
$b_{21} = -1.4739080635641988$	$b_{22} = 3.4081212175550637$	$b_{23} = -0.93421315399086491$
$b_{31} = -2.2474449407963197$	$b_{32} = 4.8389400465743577$	$b_{33} = -1.591495105778038$
$r_{11} = 0.4692939693313411$	$r_{12} = 0$	$r_{13} = 0$
$r_{21} = 0.3861200709233249$	$r_{22} = 0.4692939693313411$	$r_{23} = 0$
$r_{31} = 0.34593346278668291$	$r_{32} = 0.4946005975768783$	$r_{33} = 0.4692939693313411$
$\hat{r}_{11} = 0$	$\hat{r}_{12} = 0$	$\hat{r}_{13} = 0$
$\hat{r}_{21} = 0.49781830961253148$	$\hat{r}_{22} = 0$	$\hat{r}_{23} = 0$
$\hat{r}_{31} = 0.073011574282580455$	$\hat{r}_{32} = 0.75655848960284611$	$\hat{r}_{33} = 0$

Table 1: Coefficients of IMEX methods of order 3.

**Method 4a:**  $p = s = 4$ , A-stable, optimally zero stable

$c_1 = -0.83356855449686418$	$c_2 = 0.39925267067647718$	$c_3 = -0.22714030828660781$
$c_4 = 1$		
$b_{11} = -0.13543752646989399$	$b_{12} = -0.94681526158790538$	$b_{13} = 1.3226742791472281$
$b_{14} = -0.092555226518543643$	$b_{21} = 0.26849942748234806$	$b_{22} = 0.23343648855488061$
$b_{23} = 0.55848935956163126$	$b_{24} = -0.60425275598859907$	$b_{31} = -0.34213726582212034$
$b_{32} = -1.1311746911059599$	$b_{33} = 2.1389368012394412$	$b_{34} = 0.33437515568863896$
$b_{41} = 1.6408928968883434$	$b_{42} = 3.8669408281787074$	$b_{43} = -3.2708979617426235$
$b_{44} = -1.2369357633244271$	$r_{11} = 0.48432470456842897$	$r_{12} = 0$
$r_{13} = 0$	$r_{14} = 0$	$r_{21} = 1.23282122517334880$
$r_{22} = 0.48432470456842897$	$r_{23} = 0$	$r_{24} = 0$
$r_{31} = 0.76049048488464388$	$r_{32} = -0.15406223867438271$	$r_{33} = 0.48432470456842897$
$r_{34} = 0$	$r_{41} = 1.9894983581999484$	$r_{42} = 1.0302094135579156$
$r_{43} = -1.1861392172609913$	$r_{44} = 0.48432470456842897$	$\hat{r}_{11} = 0$
$\hat{r}_{12} = 0$	$\hat{r}_{13} = 0$	$\hat{r}_{14} = 0$
$\hat{r}_{21} = 0.66313649109206185$	$\hat{r}_{22} = 0$	$\hat{r}_{23} = 0$
$\hat{r}_{24} = 0$	$\hat{r}_{31} = 0.19514217688067359$	$\hat{r}_{32} = -0.11697155154728534$
$\hat{r}_{33} = 0$	$\hat{r}_{34} = 0$	$\hat{r}_{41} = -0.50218856665143741$
$\hat{r}_{42} = 0.75496762532404671$	$\hat{r}_{43} = 0.90081094789725258$	$\hat{r}_{44} = 0$

Table 2: Coefficients of IMEX methods of order 4.

**Remark 4.1.** *For constant stepsizes, the implicit part of method 3a is nearly superconvergent, it holds*

$$e_s^\top (I - B + \mathbb{1}e_s^\top)^{-1} AB(s + 1) = 2.5e - 8$$

whereas for method 4a is  $4.1e - 1$ . For details on superconvergence of peer methods see [14].

Figures 1 and 2 show the results of the application of the IMEX peer methods 3a and 4a to (12) for the Courant numbers  $C_A = Uh/\Delta x$  and  $C_s = c_s h/\Delta x$ . According to the construction procedure both methods are stable below the line  $C_A/C_s = U/c_s = 1/6$ , corresponding to maximal wind speed of approximately 56 m/s.

Furthermore we investigate the stability region of the found IMEX methods with respect to the linear test equation considered in [22, 23]. We applied the IMEX peer methods 3a and 4a to the test equation (13) and Figures 3 and 4 show the stability regions for these schemes.

## 5 Numerical tests

We have implemented several methods with step size control and with constant step size in MATLAB. The nonlinear systems of the implicit part in peer methods were solved by a

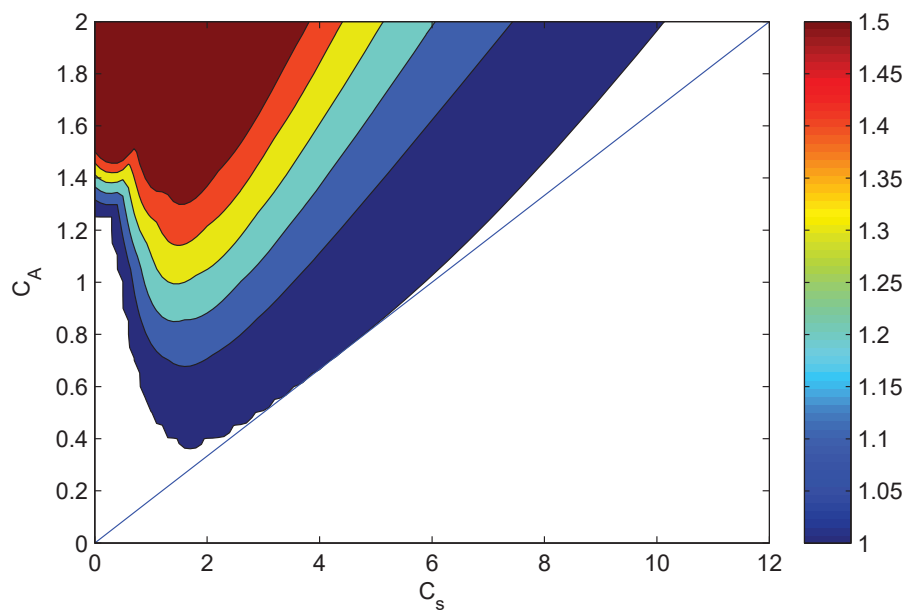


Figure 1: Stability of method **3a** for the test equation (12) .

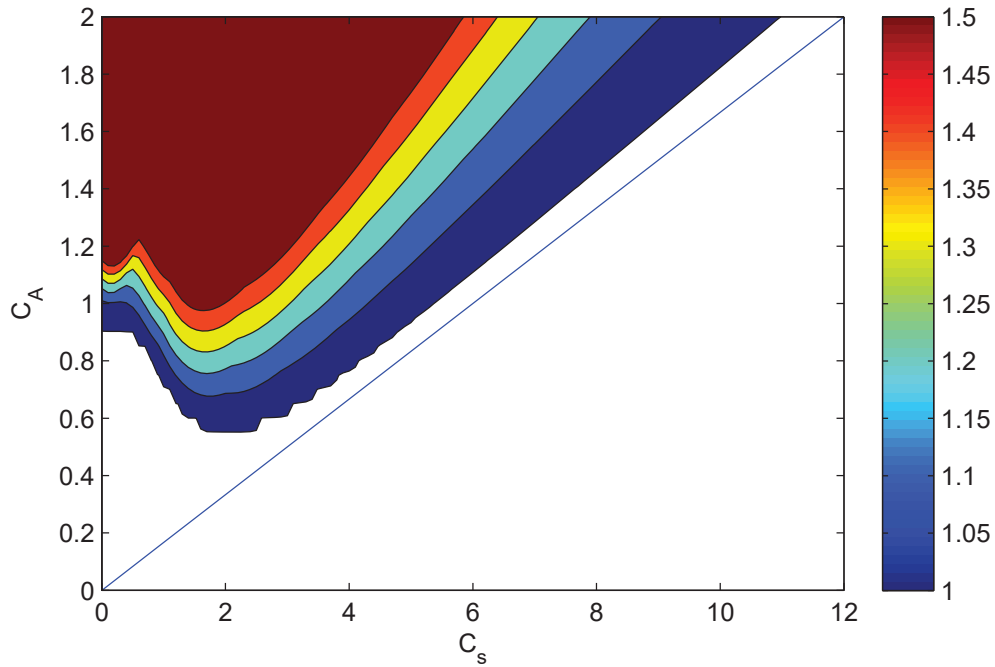


Figure 2: Stability of method **4a** for the test equation (12) .

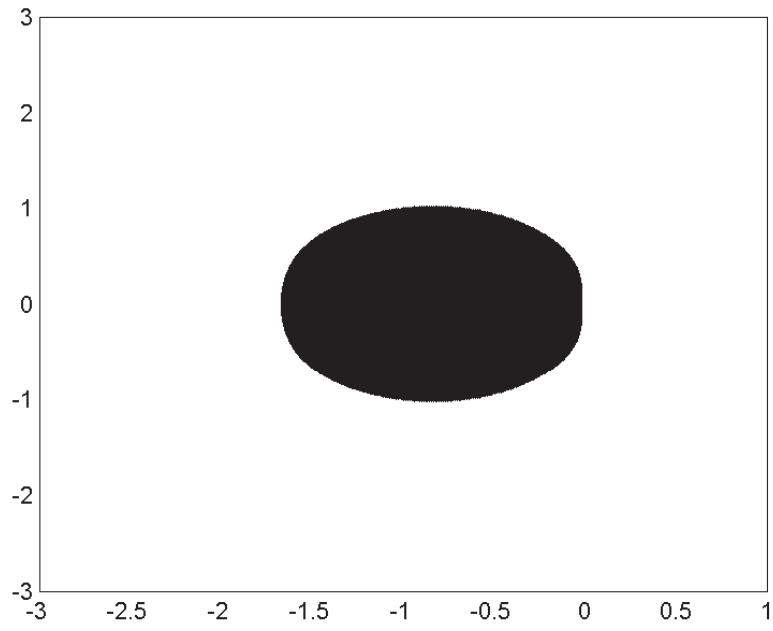


Figure 3: Stability region of method **3a** for the test equation (13) .

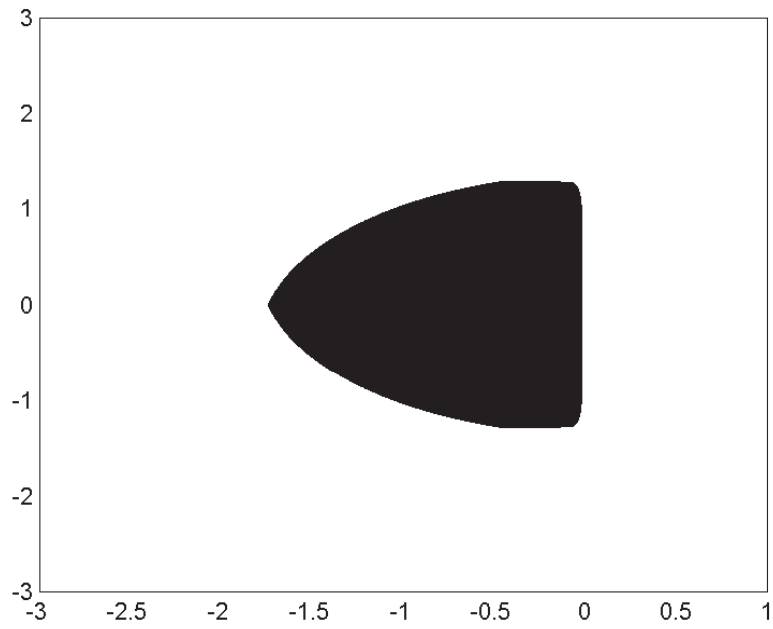


Figure 4: Stability region of method **4a** for the test equation (13) .

simplified Newton method. The iteration was stopped if

$$\max_{i=1,\dots,n} \left| \frac{\Delta y_{k,i}}{tol + tol \cdot |y_{m,i}|} \right| \leq 0.01 \cdot tol$$

where  $\Delta y_k$  is the solution of the linear system in the  $k$ -th step of the Newton process or if maximum 10 iteration steps were performed.

Here  $tol$  is the prescribed tolerance for the methods with step size control. For the methods with constant step size, we used  $tol = 0.01$  for the Newton iteration.

The following methods have been implemented:

**3a,4a** Methods from Table 1 and 2 with constant step sizes.

**3a-control,4a-control** These are methods **3a** and **4a** implemented with step size control.

**expo43** is a four stage exponential peer method of order of consistency  $p=3$ ; see [17, 19].

The free coefficients have been chosen to give good stability for the test equation (12).

Products of the form  $\varphi_l(c_i h T)v$  are approximated by Krylov-techniques using the code *phipm* of Niesen and Wright [10]. Here  $T$  stands for the Jacobian  $f_y$  of the stiff part.

**MIS4** is a four stage special split-explicit Runge-Kutta method [9] of order of consistency  $p = 3$ . It treats the nonstiff terms with a four stage explicit Runge-Kutta method and the stiff part is treated with much smaller step size by the Störmer-Verlet method.

**implicit** is the basic implicit method of **4a**. Here no splitting is done, but only the Jacobian  $f_y$  of the stiff part is used in the Newton iterations. where only the Jacobian  $f_y$  of the stiff part is used for the Newton iteration.

Note, that the results for method **MIS4** allow also a comparison of the IMEX peer methods with other methods via the tests in [21]. All methods, except **3a-control** and **4a-control** have been applied with constant step sizes.

The following problems have been considered:

## 5.1 Two dimensional nonlinear gravity waves example

In this subsection we evaluate the performance of IMEX peer methods in a nonlinear test case; see [4, 9] for more details and descriptions. The test case involves two-dimensional  $(x, z)$  nonlinear gravity waves generated by a localized region of non-divergent forcing in a stratified shear flow. With spatial coordinates given in kilometers, the background horizontal wind (in  $m/s$ ) is as follows:

$$u_0(z) = 5 + z + 0.4(5 - z)(5 + z).$$



The waves are forced by the curl of a nondivergent stream function (unit:  $m^2/s$ ):

$$\psi(x, z, t) = \psi_0 \left( \frac{\pi x}{L_x} \right) \sin(\omega t) \exp \left[ - \left( \frac{\pi x}{L_x} \right)^2 - \left( \frac{\pi z}{L_z} \right)^2 \right].$$

This example is dominated by nonhydrostatic motion and employs a grid spacing characteristic of high-resolution convective cloud models and is governed by the system

$$\begin{aligned} \frac{D}{Dt} u + \frac{\partial P}{\partial x} &= - \frac{\partial \psi}{\partial z} + \frac{u_0(z) - \bar{u}(z, t)}{\tau}, \\ \frac{D}{Dt} w + \frac{\partial P}{\partial z} &= b + \frac{\partial \psi}{\partial x}, \\ \frac{D}{Dt} b + N^2 w &= 0, \\ \frac{D}{Dt} P + c_s^2 \left( \frac{\partial u}{\partial x} + \frac{\partial w}{\partial z} \right) &= 0, \end{aligned}$$

for  $x \in [-150000, 150000]$ ,  $z \in [-5000, 5000]$  and  $t \in [0, 3000]$ .

We will investigate convergence in the time domain while keeping the spatial discretization fixed. In all simulations the numerical domain is horizontally periodic and bounded by flat rigid upper and lower surfaces. Let  $m$  and  $n$  be integer indices; the mesh is staggered so that the equation for  $P$  applies at points  $(m\Delta x, n\Delta z)$ , the equation for  $u$  applies at points  $((m - \frac{1}{2})\Delta x, n\Delta z)$ , and the equations for  $b$  and  $w$  apply at points  $(m\Delta x, (n - \frac{1}{2})\Delta z)$ . Using the operator notation

$$\begin{aligned} \delta_{nx} f(x) &= \frac{f(x + n\Delta x/2) - f(x - n\Delta x/2)}{n\Delta x}, \\ \langle f(x) \rangle^{nx} &= \frac{f(x + n\Delta x/2) + f(x - n\Delta x/2)}{2}, \end{aligned}$$

the spatial discretization has the form

$$\begin{aligned} \frac{\partial u}{\partial t} + \frac{1}{2} \delta_{2x}(u^2) + \langle \langle w \rangle^x \delta_x u \rangle^z - \frac{u_0(z) - \bar{u}(z, t)}{\tau} + K ((\Delta x \delta_x)^2 + (\Delta z \delta_z)^2)^2 u &= -\delta_x P \\ \frac{\partial w}{\partial t} + \langle \langle u \rangle^z \delta_x w \rangle^x + \frac{1}{2} \delta_{2z}(w^2) + K ((\Delta x \delta_x)^2 + (\Delta z \delta_z)^2)^2 w &= -\delta_z P + b \\ \frac{\partial b}{\partial t} + \langle \langle u \rangle^z \delta_x b \rangle^x + \langle \langle w \rangle^z \delta_z b \rangle^z + K ((\Delta x \delta_x)^2 + (\Delta z \delta_z)^2)^2 b &= -N^2 w \\ \frac{\partial P}{\partial t} + \langle u \delta_x P \rangle^x + \langle w \delta_z P \rangle^z &= -c_s^2 (\delta_x u + \delta_z w). \end{aligned}$$

where the discretized operators on the right hand side form the function  $g$ . A simple parametrization of turbulent mixing in a nearly inviscid fluid is imposed through the fourth-derivative hyper-diffusion terms. The stiff part  $f$  of (8) is given by the spatial discretization

of

$$- \begin{pmatrix} \frac{\partial P}{\partial x} \\ \frac{\partial P}{\partial z} + b \\ N^2 w \\ c_s^2 \left( \frac{\partial u}{\partial x} + \frac{\partial w}{\partial z} \right) \end{pmatrix}.$$

The nonstiff part is the rest. In our computation, we used  $nx = 100, nz = 100$  and  $nx = 600, nz = 100$  resulting the dimensions 39800 and 238800. A reference solution has been computed with the MATLAB code `ode15s` [16] with  $atol = rtol = 5 \cdot 10^{-12}$  for dimension 39800 and with the classical Runge-Kutta method of fourth order with a time step size of  $10^{-4}$  for dimension 238800.

For example with dimension 39800, the time step size (in seconds) varies over the set  $\{7.5, 15, 30, 60\}$ . For example with dimension 238800, the time step size (in seconds) varies over the set  $\{3.75, 7.5, 15, 30\}$  and for the methods with step size control we used the tolerances  $atol = rtol = tol = 10^{-1}, 10^{-2}, 10^{-3}$ .

Figure 5 shows numerical solution with method **4a-control** with tolerance  $10^{-3}$  for the horizontal velocity  $u$  field at the end point  $t_e = 3000$ ,  $x \in [-150000, 150000]$ ,  $z \in [-5000, 5000]$ ,  $nx = 600, nz = 100$ .

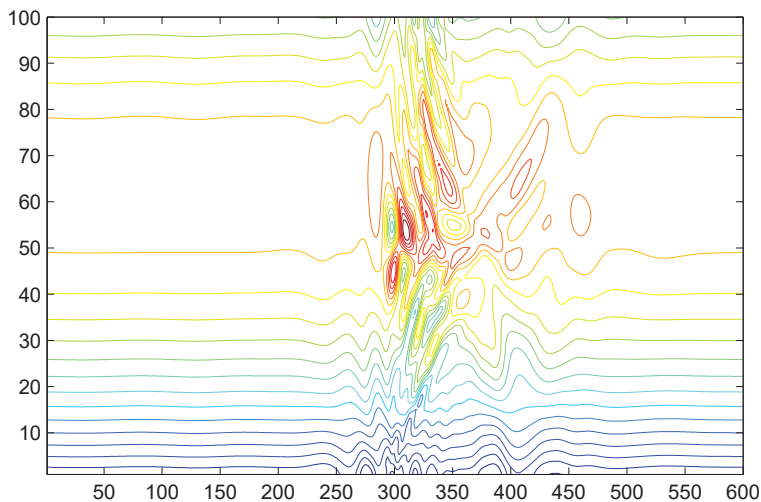


Figure 5: Contours of the horizontal velocity at the end point  $t_e = 3000$  for the grid points  $(x_i, z_i)$ .

The results for this example with dimensions 39800 and 238800 are displayed in Figures 6 and 7 respectively. The following figures show the error

$$\text{ERR} = \max_{i=1, \dots, n} \frac{|y_i - y_{\text{ref},i}|}{1 + |y_{\text{ref},i}|}$$

at the endpoint versus computing time (in seconds) where  $y$  is the numerical solution and  $y_{\text{ref}}$  is the reference solution.

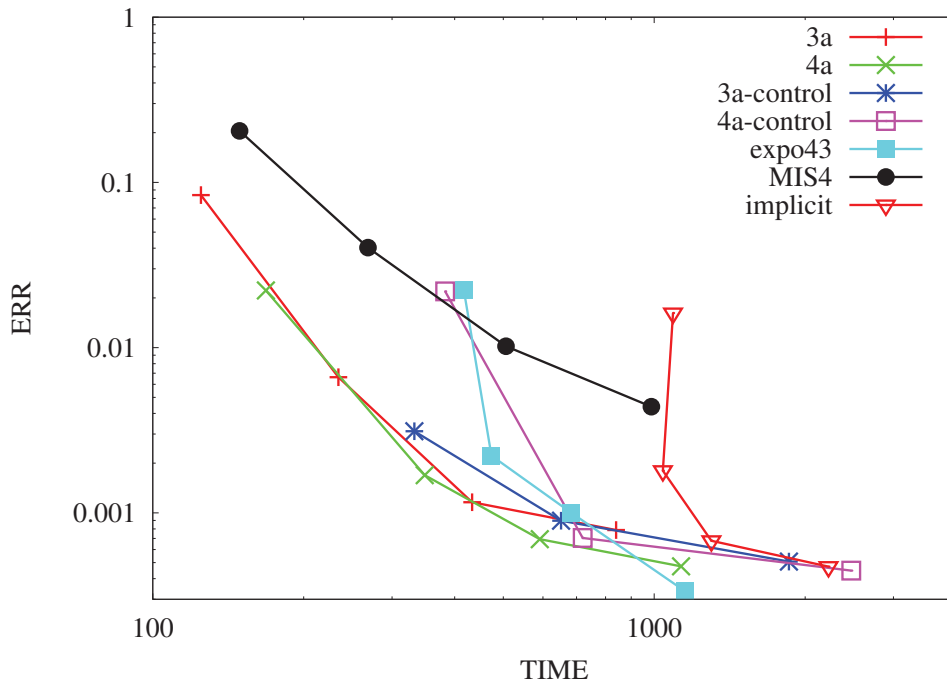


Figure 6: Results for Gravity with dimension 39880.

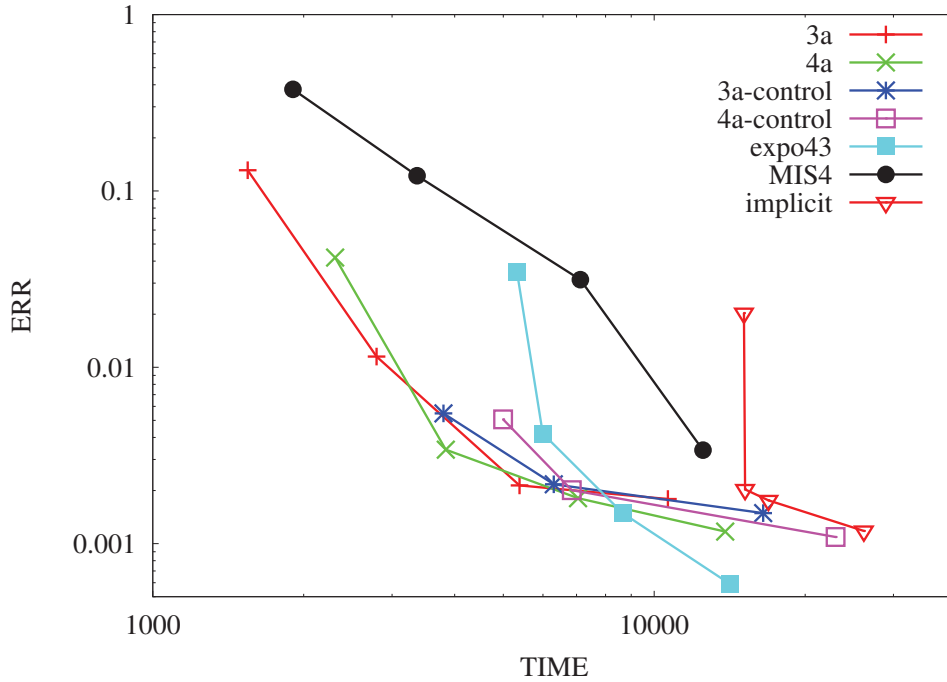


Figure 7: Results for Gravity with dimension 238800.

## 5.2 Cold bubble downburst benchmark example

In this subsection, we consider as a second example a cold bubble falling down. This example is taken from [15] with the modifications that have been made in [23].

In the modified version, a constant mean horizontal wind of  $20m/s$  is included and a periodic boundary condition in the horizontal is specified. On the ground the bubble generates winds of magnitude  $30m/s$ , several Kelvin-Helmholtz waves are generated.

A gridwidth of  $100m$  is used in both directions. With a background wind of  $20m/s$  present the maximum Mach number is slightly above  $1/6$ . Now the fully compressible Euler equations with an additional viscosity term are solved.

$$\begin{aligned}\frac{\partial \rho}{\partial t} &= -\frac{\partial \rho u}{\partial x} - \frac{\partial \rho w}{\partial z}, \\ \frac{\partial \rho u}{\partial t} &= -\frac{\partial \rho u u}{\partial x} - \frac{\partial \rho w u}{\partial z} - \frac{\partial \rho}{\partial x} + \nu[(\rho u)_{xx} + (\rho w)_{zx}], \\ \frac{\partial \rho w}{\partial t} &= -\frac{\partial \rho u w}{\partial x} - \frac{\partial \rho w w}{\partial z} - \frac{\partial \rho}{\partial z} + \nu[(\rho u)_{xz} + (\rho w)_{zz}], \\ \frac{\partial \rho \theta}{\partial t} &= -\frac{\partial \rho u \theta}{\partial x} - \frac{\partial \rho w \theta}{\partial z}.\end{aligned}$$

We have  $x \in [-10000, 10000]$ ,  $z \in [0, 10000]$  and  $t \in [0, 900]$ . The equations are discretized in space on a staggered grid, where the advection operator is approximated by third order upwinding, all other operators are approximated by second order central differencing. The resulting equations can be written in compact form

$$y' = F(y) \tag{14}$$

where  $y$  corresponds to

$$\begin{pmatrix} \rho \\ \rho u \\ \rho w \\ \rho \theta \end{pmatrix}$$

To obtain a splitting representation a linear operator  $Ly$  is introduced that approximates  $F(y)$  and contains the terms responsible for the acoustic and gravity waves.

Equation (14) is then rewritten as

$$y' = \{F(y) - Ly\} + Ly,$$

where  $f(y) = Ly$  and  $g(y) = f(y) - Ly$ . The linear operator  $Ly$  for the IMEX method is computed at  $t = t_m$  for each time step and kept constant during this time step. It is defined by the space discretization of

$$- \begin{pmatrix} \frac{\partial \rho u}{\partial x} + \frac{\partial \rho w}{\partial z} \\ \frac{\partial p}{\partial \rho} |_n \frac{\partial \rho \theta}{\partial x} \\ \frac{\partial p}{\partial \rho} |_n \frac{\partial \rho \theta}{\partial z} + g\rho \\ \frac{\partial(\rho u)\theta}{\partial x} |_n + \frac{\partial(\rho w)\theta}{\partial z} |_n \end{pmatrix} \quad (15)$$

where the values marked with  $|_n$  are fixed at some old time level, which are  $\frac{\partial p}{\partial \rho}$  in the second and third row and  $\theta$  in the last row of (15). All derivatives are discretized by central differences and necessary interpolation are done by averaging of neighbouring values. With this type of discretization the operator  $L$  has again purely imaginary eigenvalues. Note that  $L$  changes in each time step. This means that for the IMEX peer methods (11),  $F(Y_m)$  has to be adapted in the implementation. More precisely: If in the step  $t_m \rightarrow t_{m+1}$  we have

$$hRF(Y_m) = hRL_m Y_m,$$

then in the next step  $t_{m+1} \rightarrow t_{m+2}$  we will have

$$hAF(Y_m) = hAL_{m+1} Y_m,$$

i.e.,  $F(Y_m)$  will change.

Snapshots of the numerical solutions with method **4a-control** with tolerance  $10^{-4}$  at  $t = 0s$ ,  $t = 450s$  and  $t = 900s$  are displayed in Figure 8.

For this example, the time step size varies over the set  $\{0.125, 0.25, 0.5, 1\}$  and for the methods with step size control we used the tolerances  $atol = rtol = tol = 10^{-1}, 10^{-2}, \dots, 10^{-4}$ . The reference solution has been computed with **ode15s** with  $atol = rtol = 5 \cdot 10^{-10}$ .

## 6 Conclusion

The results show that IMEX peer methods are reliable and accurate. In the test problems, the most expensive part is the nonstiff part, which is computed with an explicit peer method.

For the gravity waves example, the methods **3a** and **4a** are clearly superior for crude and middle accuracies. For more strict accuracies, **expo43** and the implementation of methods **3a** and **4a** with step size control become competitive. **MIS4** and the **implicit** method are outperformed by the IMEX peer methods.

For the cold bubble downburst example, the results are similar. However here **expo43** becomes competitive already for middle accuracies and is superior for high accuracies.

We believe that the much higher accuracy of the IMEX peer methods compared with **MIS4** is due the high stage order of the peer methods.

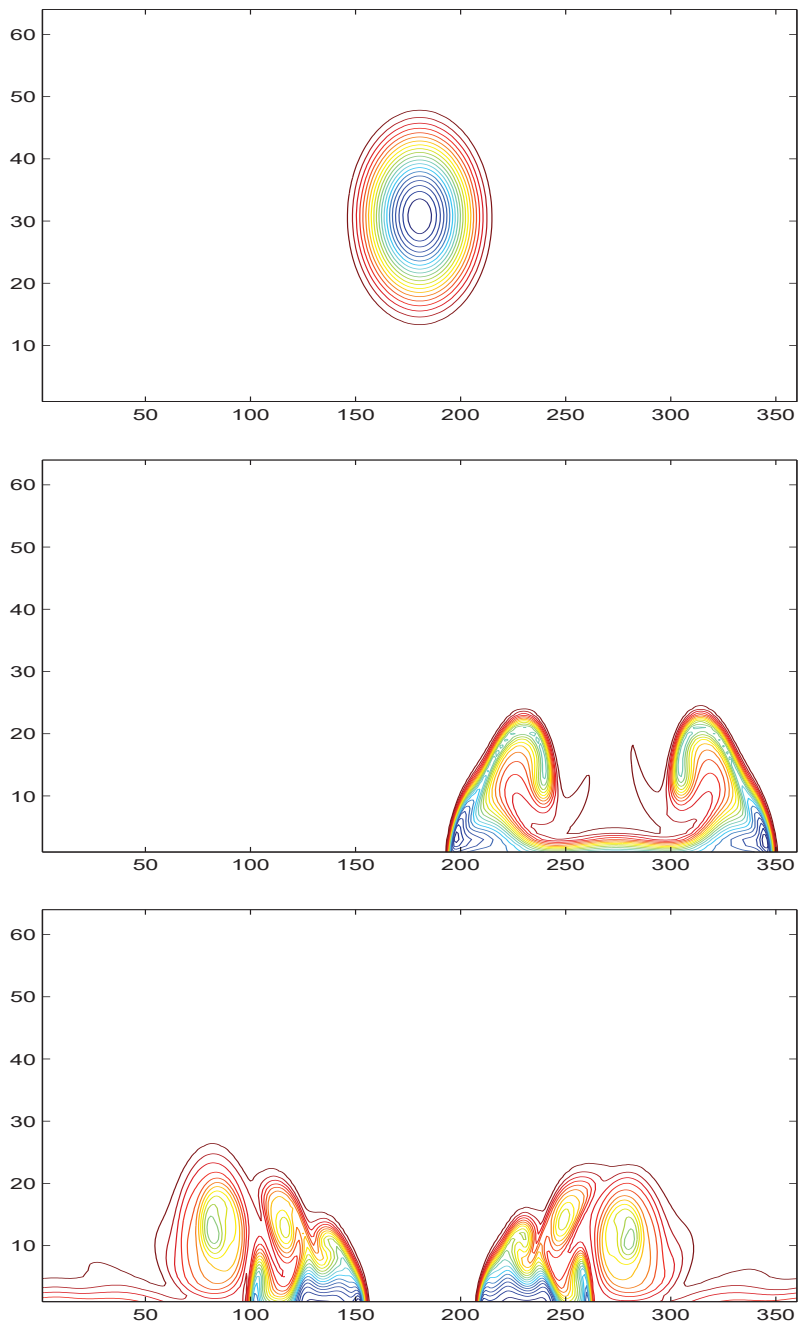


Figure 8: Potential temperature deviation of background state at the beginning, the middle and the end of the simulation computed with method **4a-control** with tolerance  $10^{-4}$  at  $t = 0s$ ,  $t = 450s$  and  $t = 900s$ .

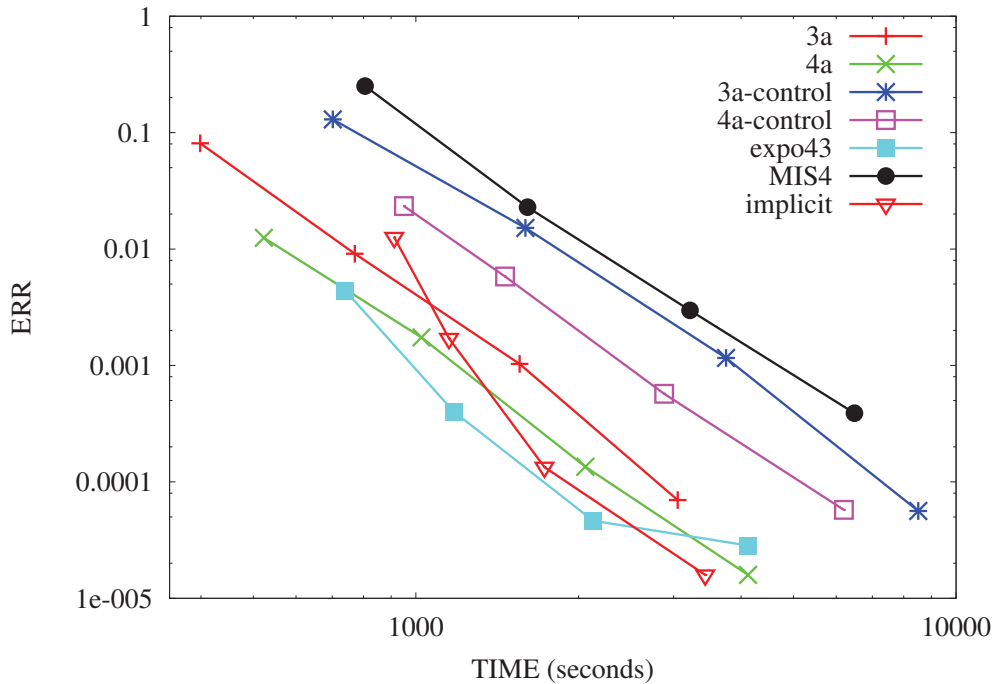


Figure 9: Results for the Bubble problem.

The results show that IMEX peer methods are well suited for problems with stiff and nonstiff terms. Due to their high stage order  $q$ , IMEX peer methods can be constructed straightforwardly by combining explicit and implicit peer methods of order  $p = q$ . The coefficients of the method can easily be adapted to the requirements of the special problem class, like to the stability requirements of fast-wave-slow-wave problems in this paper.

## References

- [1] U.M. Ascher, S.J. Ruuth, R.J. Spiteri, *Implicit-explicit Runge-Kutta methods for time-dependent partial differential equations*, Appl. Num. Math. 25 (1997), 151–167.
- [2] S. Beck, S. Gonzalez-Pinto, S. Perez-Rodriguez and R. Weiner, *A comparison of AMF- and Krylov-methods in MATLAB for large stiff ODE systems*, J. Comput. Appl. Math. 262 (2014), 292–303.
- [3] S. Beck, R. Weiner, H. Podhaisky, B.A. Schmitt, *Implicit parallel peer methods for large stiff ODE systems*, Appl. Math. Comput. 38 (2012), 389–406.
- [4] D.R. Durran and P.N. Blossey, *Implicit-explicit multistep methods for fast-wave-slow-wave problems*, Mon. Wea. Rev., 140 (2012), 1307–1325.

- [5] A. Gerisch, J. Lang, H. Podhaisky and R. Weiner, *High-order linearly implicit two-step peer—finite element methods for time-dependent PDEs*, Appl. Numer. Math., 59 (2009), 624–638.
- [6] F. X. Giraldo, J. F. Kelly and E. M. Constantinescu, *Implicit-explicit formulations of a three-dimensional nonhydrostatic unified of the atmosphere (NUMA)*, SIAM J. Sci. Comput., 35(5) (2013), B1162–B1194.
- [7] D. Ghosh and E. M. Constantinescu, *Semi-implicit Time Integration of Atmospheric Flows with Characteristic-Based Flux Partitioning*, SIAM J. Sci. Comput., 38(3) (2016), A1848–B1875.
- [8] S. Jebens, O. Knoth and R. Weiner, *Explicit Two-Step Peer Methods for the Compressible Euler Equations*, Monthly Weather Review, 137 (2008), 2380–2392.
- [9] O. Knoth, J. Wensch, *Generalized Split-Explicit Runge-Kutta Methods for the Compressible Euler Equations*, Monthly Weather Review, 142 (2014), 2067–2081.
- [10] J. Niesen, W. Wright, *A Krylov subspace algorithm for evaluating the  $\varphi$ -functions appearing in exponential integrators*, ACM TOMS. 38(3) (2012), 22.
- [11] H. Podhaisky, R. Weiner, B.A. Schmitt, *Rosenbrock-type 'Peer' two-step methods*, Appl. Numer. Math. 53 (2005), 409–420.
- [12] B.A. Schmitt, R. Weiner, K. Erdmann, *Implicit parallel peer methods for stiff initial value problems*, Appl. Numer. Math. 53 (2005), 457–470.
- [13] B.A. Schmitt, R. Weiner, H. Podhaisky, *Multi-implicit peer two-step W-methods for parallel time integration*, BIT Numer. Math. 45 (2005), 197–217.
- [14] B.Soleimani, R. Weiner, *A class of implicit peer methods for stiff systems*, J. Comput. Appl. Math. (2016), doi:10.1016/j.cam.2016.06.014.
- [15] J.M. Straka, R.B. Wilhelmson, L.J. Wicker, J.R. Anderson and K.K. Droegemeier, *Numerical solutions of a non-linear density current: A benchmark solution and comparisons*, Int. J. Numer. Methods Fluids, 17 (1993), 1–22.
- [16] L. F. Shampine and M. W. Reichelt, *The MATLAB ODE suite*, SIAM J. Sci. Comput., 18 (1997), 1–22.
- [17] R. Weiner, J. Bruder, *Exponential Krylov peer integrators*, BIT Numer. Math. 56 (2016), 375–393.
- [18] R. Weiner, K. Biermann, B.A. Schmitt, H. Podhaisky, *Explicit two-step peer methods*, Computers and Mathematics with Application. 55(4) (2008), 609–619.
- [19] R. Weiner, T. El-Azab, *Exponential Peer Methods*, Appl. Numer. Math. 62 (2012), 1335–1348.



- [20] R. Weiner, B.A. Schmitt, H. Podhaisky, S. Jebens, *Superconvergent explicit two-step peer methods*, J. Comput. Appl. Math. 223 (2009), 753–764.
- [21] J. Wensch, O. Knöth, A. Galant, *Multirate infinitesimal step methods for atmospheric flow simulation*, BIT Numer. Math. 49 (2009), 449–473.
- [22] L.J. Wicker, W. Skamarock, *A time-splitting scheme for the elastic equations incorporating second order Runge-Kutta time differencing*, Mon. Weather Rev. 126 (1998), 1992–1999.
- [23] L.J. Wicker, W. Skamarock, *Time splitting methods for elastic models using forward time schemes*, Mon. Weather Rev. 130 (2002), 2088–2097.
- [24] H. Zhang, A. Sandu, S. Blaise, *Partitioned and Implicit-Explicit general linear methods for ordinary differential equations*, J. Sci. Comput. 61 (2014), 119–144.
- [25] E. Zharovsky, A. Sandu, H. Zhang, *A class of implicit-explicit two-step Runge-Kutta methods*, SIAM J. Numer. Anal. 53 (2015), 321–341.



## Reports of the Institutes 2016

**01-16.** M. Arnold, *DAE aspects of multibody system dynamics*

**02-16.** B. Soleimani and Chr. Tammer, *A Vector-Valued Ekeland's Variational Principle in Vector Optimization with Variable Ordering Structures*

**03-16.** R. Weiner, H. Podhaisky and M. Klinge, *Explicit peer methods with variable nodes*